Supplemental Figures for

Evolutionary rewiring of the wheat transcriptional regulatory network by lineage-specific transposable elements

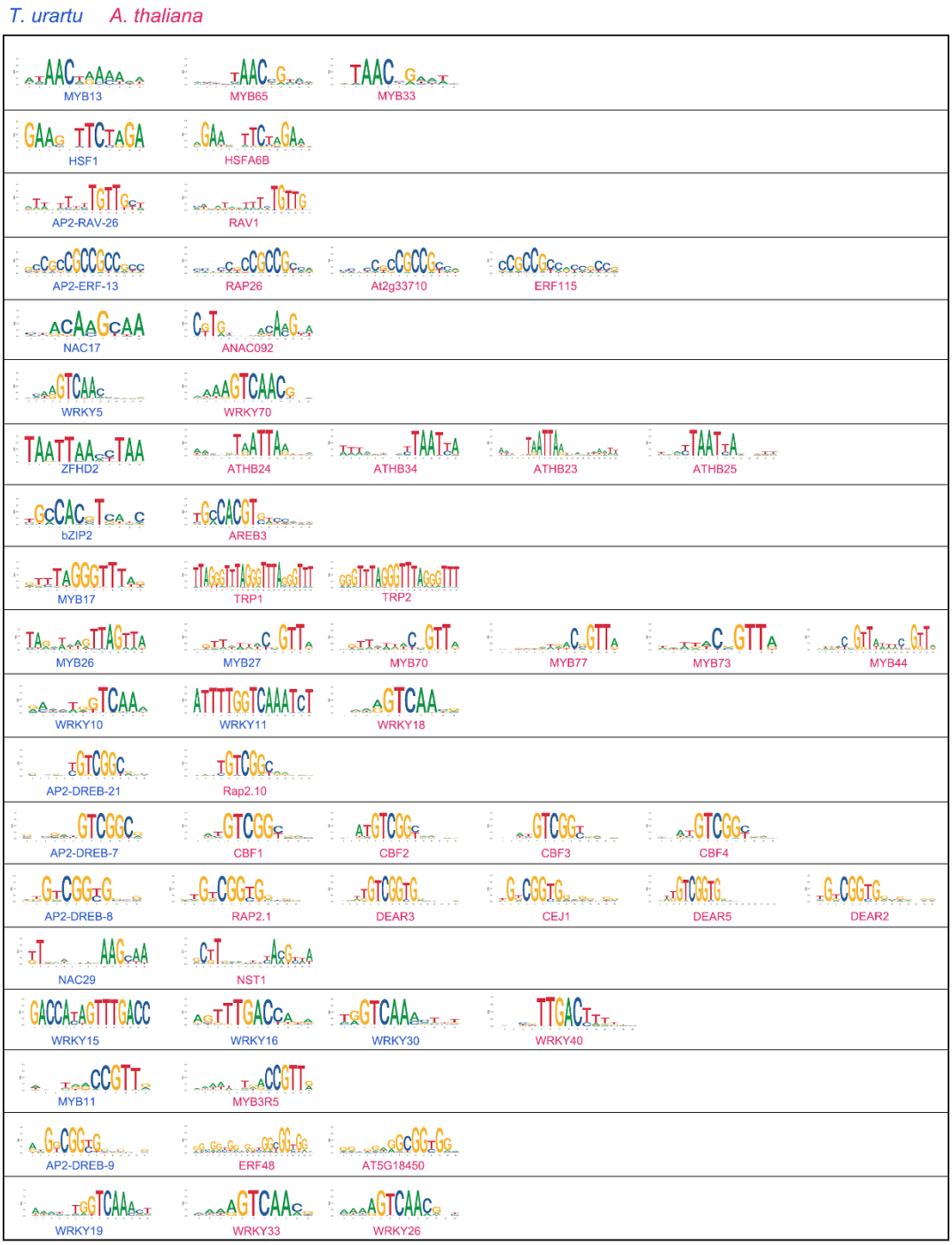

Supplemental Figure S1. The motifs *de novo* identified from DAP-seq peaks in *T. urartu* (blue) and the motifs of homologous TFs in *A. thaliana* (red) from JASPAR database. TFs within the same ortholog group were arranged in the same row.

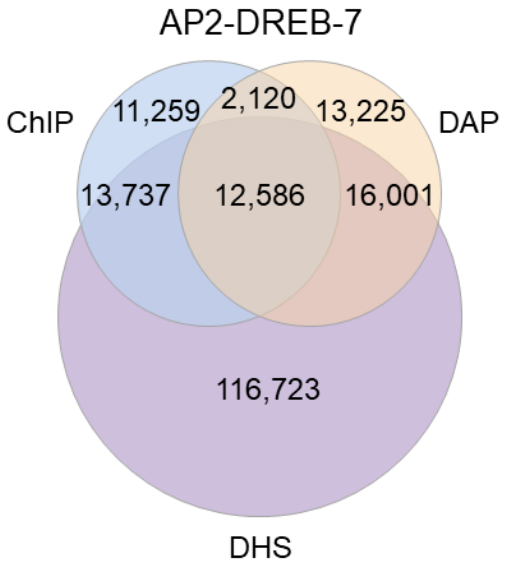

Supplemental Figure S2. The Venn plot shows the overlap between DAP-seq and ChIP-seq of AP2-DREB-7 with DHS.

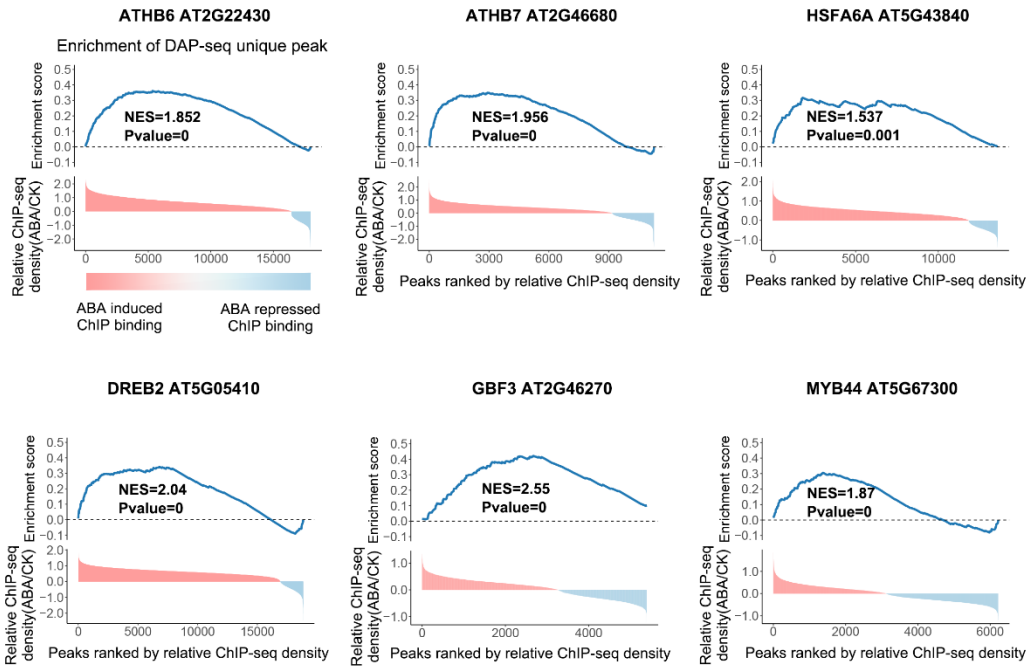

Supplemental Figure S3. Enrichment of DAP-seq peaks in ChIP-seq ABA responsive peaks in *A. thaliana*.

Top panel: ChIP-seq density distribution of ABA responsive TFs before and after ABA treatment in DAP-seq unique peaks. Bottom panel: Enrichment of DAP-seq unique peaks (DAP-CK vs ChIP-CK) in ABA-induced ChIP-seq binding. GSEA was applied for calculating enrichment statistics. X-axis, peaks were ranked by the relative ChIP-seq density with and without ABA treatment. ABA increased ChIP binding are on the left, and ABA reduced ChIP binding are on the right. Y-axis for the lower panel is the log2 fold change of ChIP-seq read densities with and without ABA treatment. Y-axis for the upper panel represent the relative enrichment of DAP-seq unique peaks in ChIP-seq peaks designated by X-axis. Numeric values show normalized enrichment score and the *P* value.

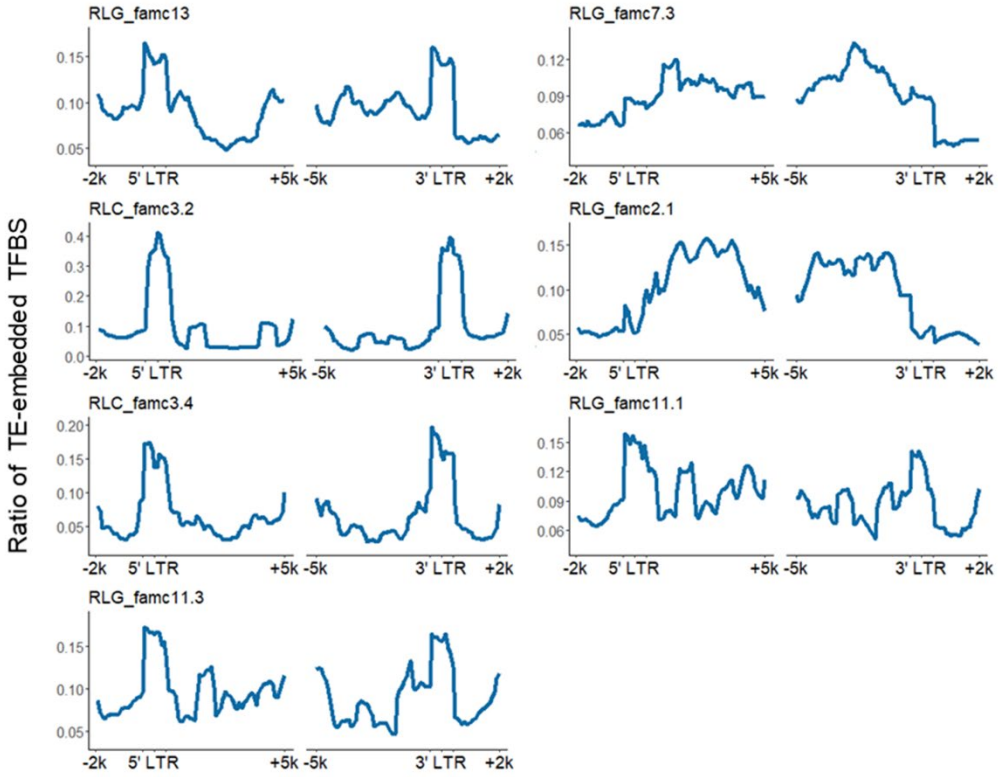

Supplemental Figure S4. Profiles of TE-embedded TFBS distribution in full-length Gypsy LTRs top enriched in Fig. 4G.

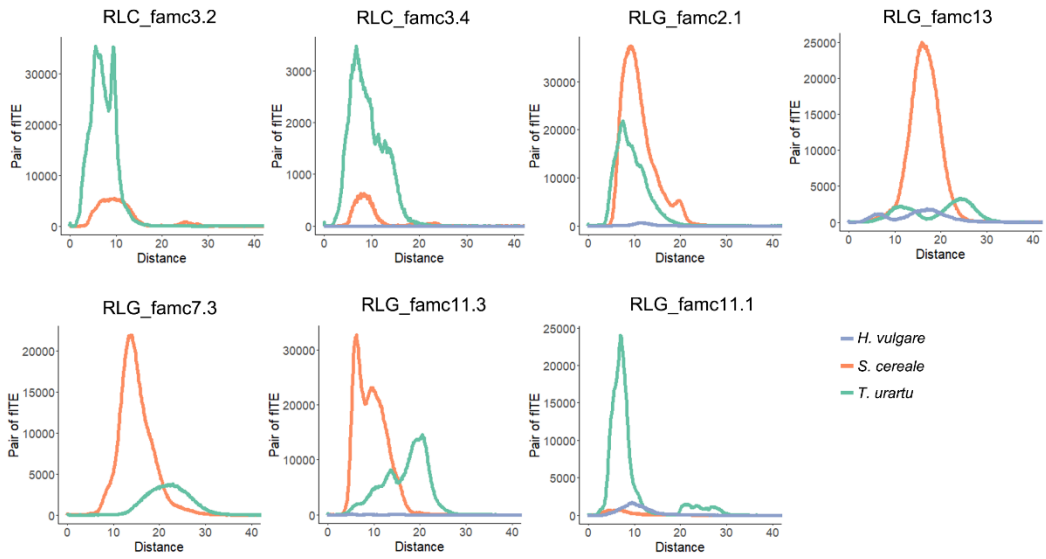

Supplemental Figure S5. Frequency distribution of full-length TE sequence divergence of each TE subfamily in *H. vulgare*, *S. cereale* and *T. urartu*.

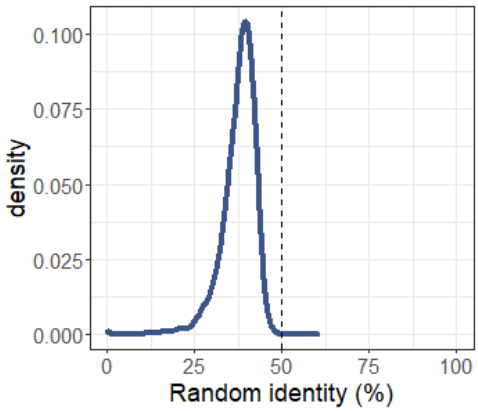

Supplemental Figure S6. The distribution of alignment identity between randomly selected TE-embedded TFBS and non-TE TFBS pairs. The cutoff of 50% is significantly higher than random pairs.

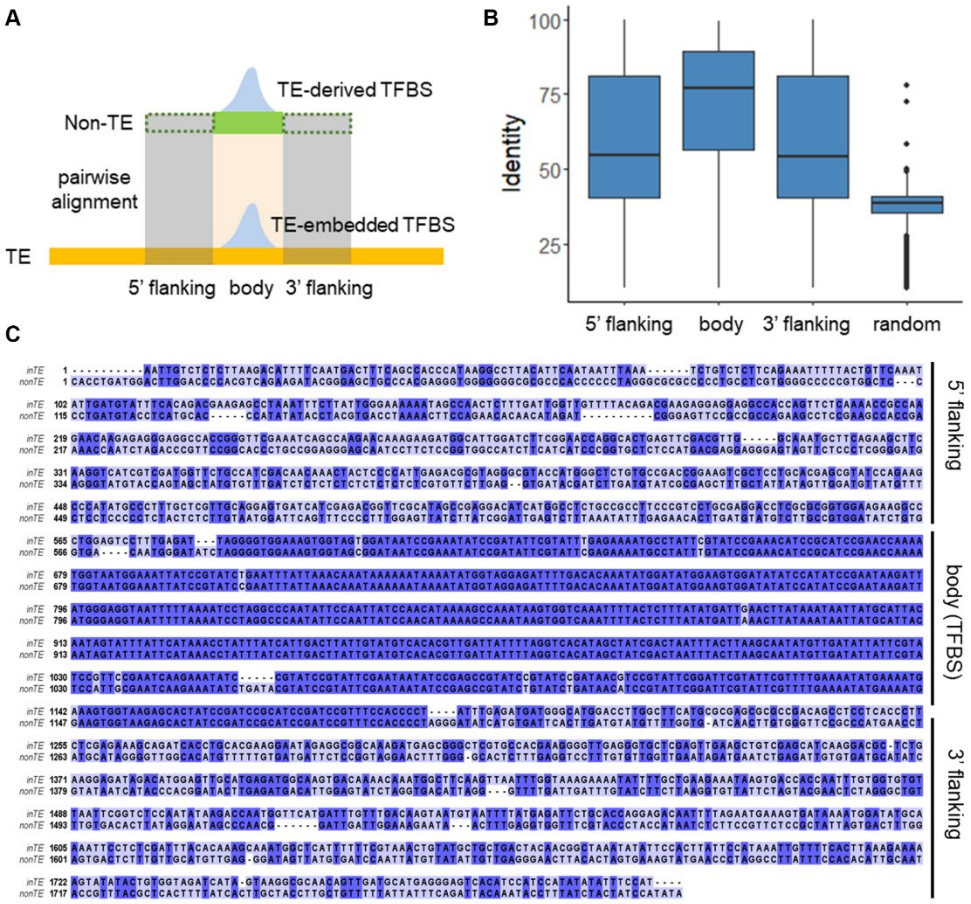

Supplemental Figure S7. Pairwise sequence alignment of the body and flanking regions between the TE-derived TFBSs and the source TE-embedded TFBSs.

A, Schematic of pairwise alignment. The length of body and flanking regions are both 600 bp.

B, Pairwise alignment identity of the body and flanking regions. TE-embedded TFBSs and randomly selected non-TE regions were also aligned.

C, The alignment result of a TE-embedded and TE-derived pair. The genomic location of TE-embedded (inTE) region is “Tu5:458412882-458414683(+)” and the TE-derived region(nonTE) is “Tu7:710903151-710904952(+)”.

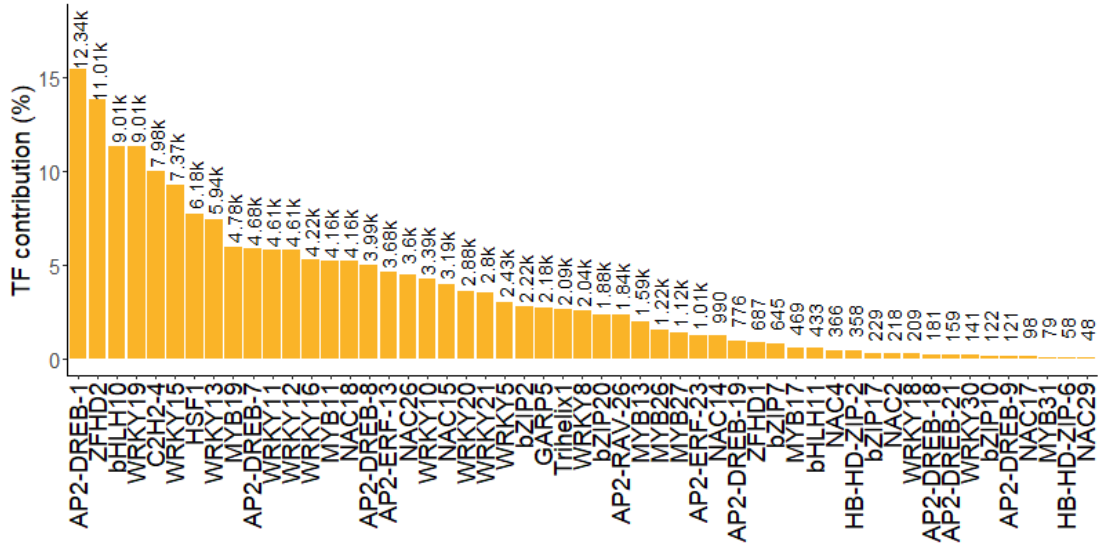

Supplemental Figure S8. Contribution of each TF in TE-derived TFBS.

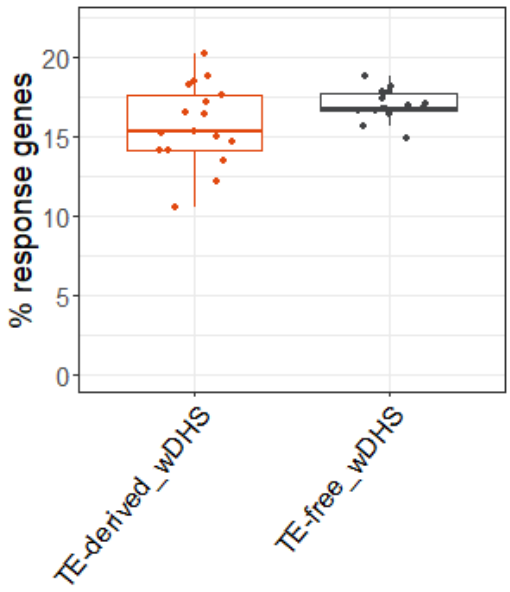

Supplemental Figure S9. The comparation of stress responsive target genes between TE-derived and TE-free TFBS overlapping DHS.

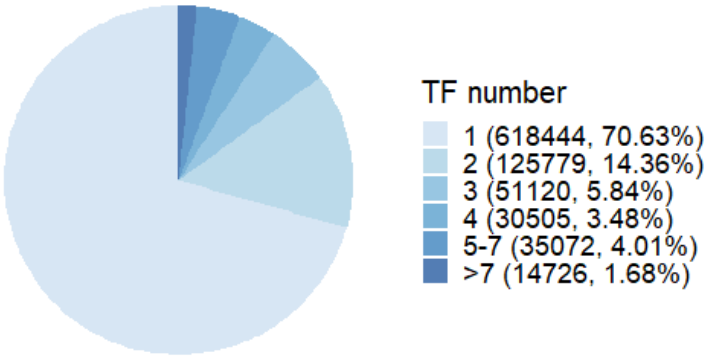

Supplemental Figure S10. Distribution of the merged TFBS with different numbers of TFs.